

Damping dependence in dynamic magnetic hysteresis of single-domain ferromagnetic particles

H. El Mrabti,¹ P. M. Déjardin,¹ S. V. Titov,² and Yu. P. Kalmykov^{1,*}

¹Laboratoire de Mathématiques et Physique (EA 4217), Université de Perpignan Via Domitia, F-66860, Perpignan, France

²Kotel'nikov's Institute of Radio Engineering and Electronics, Russian Academy of Sciences, 1, Vvedenskii Square, Fryazino, 141190, Russia

(Received 4 November 2011; revised manuscript received 9 March 2012; published 26 March 2012)

It is demonstrated that both the area of the dynamic magnetic hysteresis (DMH) loop and the volume power loss of an assembly of uniaxial superparamagnetic nanoparticles with a random distribution of easy axes are very sensitive to damping at low, intermediate, and high frequencies. In particular, a dynamical regime that is resonant in character occurs in the vicinity of the ferromagnetic resonance (FMR) frequency for low to moderate values of the alternating current (ac) field amplitude. The resonant regime is characterized by a diamagnetic-like response of the particles, resulting from a phase lag of the stationary nonlinear magnetization with respect to the applied field greater than $\pi/2$.

DOI: 10.1103/PhysRevB.85.094425

PACS number(s): 75.50.Tt, 75.20.-g, 75.60.Ej, 75.75.Jn

I. INTRODUCTION

The dynamic magnetic hysteresis (DMH) induced in fine magnetic particles by an external alternating current (ac) field constitutes a topic of substantial interest since the phenomenon occurs in magnetic information storage and magnetodynamic hyperthermia occasioned by induction heating of nanoparticles.¹⁻³ Superparamagnetism, which plays a crucial role in the magnetodynamics of nanoparticles, naturally emphasizes the physics of DMH, since in superparamagnetic particles, the temperature directly influences the remagnetization conditions, strongly affecting the effective rates, and so altering the loop shape, coercive force, and specific power loss.

The theory of DMH in single-domain magnetically isotropic particles subjected to thermal fluctuations, having been proposed by Ignachenko and Gekht,⁴ was later extended to uniaxial superparamagnetic particles with moderate to high internal barriers.⁵⁻⁷ These approaches all stem from Brown's treatment of thermal fluctuations of the magnetization of a single-domain ferromagnetic particle⁸ inspired by Néel.⁹ By setting the theory firmly in the context of classical Brownian motion, Brown derived the Fokker-Planck equation for the probability density function W of the magnetization orientations on a sphere of unit radius. This equation is

$$2\tau_N \frac{\partial}{\partial t} W = \beta[\alpha^{-1} \mathbf{u} \cdot (\nabla V \times \nabla W) + \nabla \cdot (W \nabla V)] + \nabla^2 W, \quad (1)$$

where $\mathbf{u} = \mathbf{M}/M_S$ is a unit vector along the magnetization vector \mathbf{M} , M_S is the saturation magnetization (assumed constant for a given temperature), $\nabla = \partial/\partial \mathbf{u}$ is the gradient operator on the unit sphere, V is the free-energy density, $\beta = v/(kT)$, v is the volume of the particle, k is Boltzmann's constant, T is the absolute temperature, $\tau_N = \beta M_S(1 + \alpha^2)/(2\alpha\gamma)$ is the free (i.e., for $V = 0$) rotational diffusion time of the magnetization, γ is the gyromagnetic ratio, and α is a phenomenological dimensionless damping constant (in principle, it is possible to estimate α experimentally by measuring the decay rate, the mean excess energy, or the line width in the magnetic resonance of superparamagnets¹⁰). In general, the damping strength influences strongly the magnetization dynamics of superparamagnets, leading to substantial damping dependence of all their dynamic characteristics such as the DMH.

Nevertheless, damping effects in the DMH of superparamagnets have received little attention.

Now, the determination of the DMH from Eq. (1) for arbitrary ac field strengths always involves nonlinear response of the magnetization. In the most rudimentary model, the free-energy density V of a superparamagnetic nanoparticle with uniaxial anisotropy in superimposed homogeneous external magnetic direct current (dc) and ac fields $\mathbf{H}_0 + \mathbf{H} \cos \omega t$ of arbitrary strengths and orientations with respect to the easy axis has the form

$$\beta V = \sigma \sin^2 \vartheta - \xi_0 \mathbf{u} \cdot \mathbf{H}_0/H_0 - \xi \cos \omega t \mathbf{u} \cdot \mathbf{H}/H, \quad (2)$$

where $\sigma = \beta K$, K is the anisotropy constant, $\xi_0 = \beta M_S H_0$ and $\xi = \beta M_S H$ are the dimensionless external field parameters, and ϑ is the polar angle. For an ac field of arbitrary strength, efficient numerical algorithms have been proposed by Raikher *et al.*¹¹ and Déjardin *et al.*,¹² yielding the nonlinear magnetic susceptibility, the nonlinear ferromagnetic resonance (FMR), and nonlinear DMH. However, their calculations were restricted to fields aligned along the easy axis of the particle. Although the latter assumption simplifies the calculations because the problem becomes axially symmetric, it is hardly realizable under experimental conditions. Moreover, many interesting nonlinear effects (such as the damping dependence of the DMH loop area, the interplay between thermoactivation and precession, etc.) cannot be treated and consequently understood because no dynamical coupling between the longitudinal and transverse (precessional) modes exists. Conversely, the nonlinear dynamical response of a uniaxial superparamagnet in an ac field applied at an angle to the easy axis is very sensitive to damping in the underdamped range, $\alpha < 1$, due to the coupling now induced by the driving field between the precession of the magnetization and its thermoactivation over the potential barrier.¹³⁻¹⁵ Recently, Poperechny *et al.*¹⁶ elaborated a numerical method for the calculation of the nonlinear ac stationary response, and they presented detailed results for the temperature and frequency dependence of the nonlinear DMH of uniaxial superparamagnets with randomly oriented easy axes. However, they neglected the gyromagnetic term in Eq. (1), so that their results apply only in the intermediate to high damping (IHD) range, $\alpha \geq 1$, and low frequencies, where precessional effects may be ignored. Now,

an effective numerical algorithm for the calculation of the nonlinear ac stationary response *valid in wide damping and all frequency ranges* for both an individual nanoparticle and an assembly of noninteracting particles has been given by Titov *et al.*¹⁷ In particular, they demonstrated that the usual assumption that the strong external fields are applied along the easy axis yields a poor description of the response of an assembly of randomly oriented nanoparticles; however, they also showed that for the linear response, this assumption may be retained by defining an *effective anisotropy parameter*. Here, we shall evaluate via the method developed in Ref. 15 the *damping dependence* of the DMH of an assembly of noninteracting uniaxial superparamagnetic nanoparticles with randomly oriented easy axes.

II. BASIC EQUATIONS

Now, the DMH loop represents a parametric plot of the steady-state time-dependent magnetization as a function of the ac field, i.e., $M_H(t)$ vs. $H(t) = H \cos \omega t$. The steady-state magnetization $M_H(t)$ of the assembly is given by (we shall suppose for simplicity that the dc field $\mathbf{H}_0 = 0$)¹⁵

$$M_H(t) = M_S \sum_{k=-\infty}^{\infty} \overline{m_1^k} e^{ik\omega t}, \quad (3)$$

where

$$m_1^k = \sqrt{\frac{4\pi}{3}} \left[c_{1,0}^k \cos \psi + \frac{c_{1,-1}^k - c_{1,1}^k}{\sqrt{2}} \sin \psi \right],$$

ψ is the angle between \mathbf{H} and the Z axis, which is taken as the easy axis of the particle, the overbar denotes averaging over easy-axis orientations (see Appendix), $c_{n,m}^k$ are the frequency-dependent Fourier coefficients in the Fourier expansion of the probability distribution function $W(\vartheta, \varphi, t)$ in Eq. (1), viz.,

$$W(\vartheta, \varphi, t) = \sum_{n=0}^{\infty} \sum_{m=-n}^n \sum_{k=-\infty}^{\infty} c_{n,m}^k Y_{n,m}(\vartheta, \varphi) e^{ik\omega t}, \quad (4)$$

and $Y_{n,m}(\vartheta, \varphi)$ is a spherical harmonic of order n and rank m . The numerical method of calculation of $c_{n,m}^k$ using matrix continued fractions (MCFs) is described in detail in Ref. 15 (see Appendix). Furthermore, we can calculate the normalized area of the DMH loop A_n (which is the energy loss per particle and per cycle of the ac field), defined as⁶

$$A_n = \frac{1}{4M_S H} \oint M_H(t) dH(t) = -\frac{\pi}{4} \text{Im}(\overline{m_1^1}). \quad (5)$$

This is related to the volume power loss R via $R = 2vM_S H \omega A_n / \pi$.⁶

For a weak ac field ($\xi \rightarrow 0$), $\chi(\omega) = 2\overline{m_1^1}/\xi$ defines the linear dynamic susceptibility.^{14,15} Here, the behavior of the DMH can be readily understood because at low frequencies, $\chi(\omega)$ can be described by the Debye-like formula⁹

$$\frac{\chi(\omega)}{\chi(0)} \approx \frac{1}{1 + i\omega\tau}, \quad (6)$$

where τ is the reversal time in the absence of the ac and dc fields, and τ can be estimated from Brown's formula for the

axially symmetric potential $\sigma \sin^2 \vartheta$, namely,⁶

$$\tau \sim \tau_0 \frac{(1 + \alpha^2)}{2\alpha} \sqrt{\frac{\pi}{\sigma}} e^\sigma, \quad (7)$$

where $\tau_0 = M_S / (2\gamma K)$ is a characteristic relaxation time (with typical estimations $\tau_0 \sim 10^{-10}$ s and $\tau \sim 1.2 \times 10^{-8} \div 2 \times 10^{-2}$ s for $\sigma \sim 5 \div 20$ and $\alpha \sim 1$). Then, noting that

$$\frac{M_H(t)}{M_H(0)} \approx \frac{\cos \omega t + \omega\tau \sin \omega t}{1 + \omega^2\tau^2}, \quad (8)$$

and introducing the reduced variables $x(t) = H(t)/H$ and $y(t) = M_H(t)/M_H(0)$, we have the equation of an ellipse in the (x, y) plane, namely,⁶

$$x^2 + \frac{1}{\omega^2\tau^2} [(1 + \omega^2\tau^2)y - x]^2 = 1. \quad (9)$$

This ellipse is centered at $(0, 0)$, and its major axis is tilted at an angle $\frac{1}{2} \arctan[2/(\omega\tau)^2]$.⁶ For strong ac field amplitudes, where analytical formulas for $M_H(t)$ are not available, DMH loops exhibit a variety of complicated shapes with a pronounced frequency and temperature dependence¹⁶; nevertheless, their qualitative behavior can be understood.

III. RESULTS AND DISCUSSION

Here, we focus our attention on the damping dependence of the DMH loop, DMH area, and specific power loss at low ($\omega\tau \leq 1$), intermediate ($\tau^{-1} < \omega < 0.2\omega_{\text{FMR}}$), and FMR ($\omega \sim \omega_{\text{FMR}}$) frequencies. For moderate barrier heights ($\sigma = 5$), DMH loops in the quasistatic ($\omega\tau_0 = 0.001$) and intermediate ($\omega\tau_0 = 0.1$) frequencies for various α are shown in Fig. 1. One may discern from Figs. 1(a) and 1(b) the variation of the coercive force of the assembly with damping under quasistatic conditions. As the damping is increased, the coercive force is reduced until $\alpha = 1$, where the average reversal time attains a minimum. Then, the coercive force increases again in unbounded fashion, while the remanent field increases until α reaches the critical value $\alpha_{\text{cr}} \approx (2\omega\tau_0)^{-1}$. This value of α actually delineates the limit of the switching regime. If $\alpha > \alpha_{\text{cr}}$, one encounters the “kinetic freezing” regime,¹⁶ where the motion of the magnetization is so overdamped that the magnetization vector barely departs from its initial orientation in spite of the energetically unfavorable situation. The DMH loop then flattens, merging progressively with the field axis at $\alpha \gg 1$. In the IHD damping range ($\alpha \geq 1$), the gyromagnetic term in the Fokker-Planck equation Eq. (1) can be ignored in the calculation of the coercive force of an assembly of nanoparticles with randomly distributed easy axes in this DMH regime.

As shown by Poperechny *et al.*,¹⁶ the kinetic picture of DMH is essentially quite different from the Stoner-Wohlfarth one. At low frequencies, where the field changes are quasi-adiabatic, the dynamic magnetization regime represents the so-called switching regime, meaning that the magnetization may reverse due to the cooperative shuttling action of thermal agitation and applied field. For low (but finite) damping, this results in a coercive force smaller than the Stoner-Wohlfarth value $h_{\text{SW}} = 0.48$. Furthermore, the remanent field is also smaller than the Stoner-Wohlfarth one $m_r^{\text{SW}} = 0.5$. This may

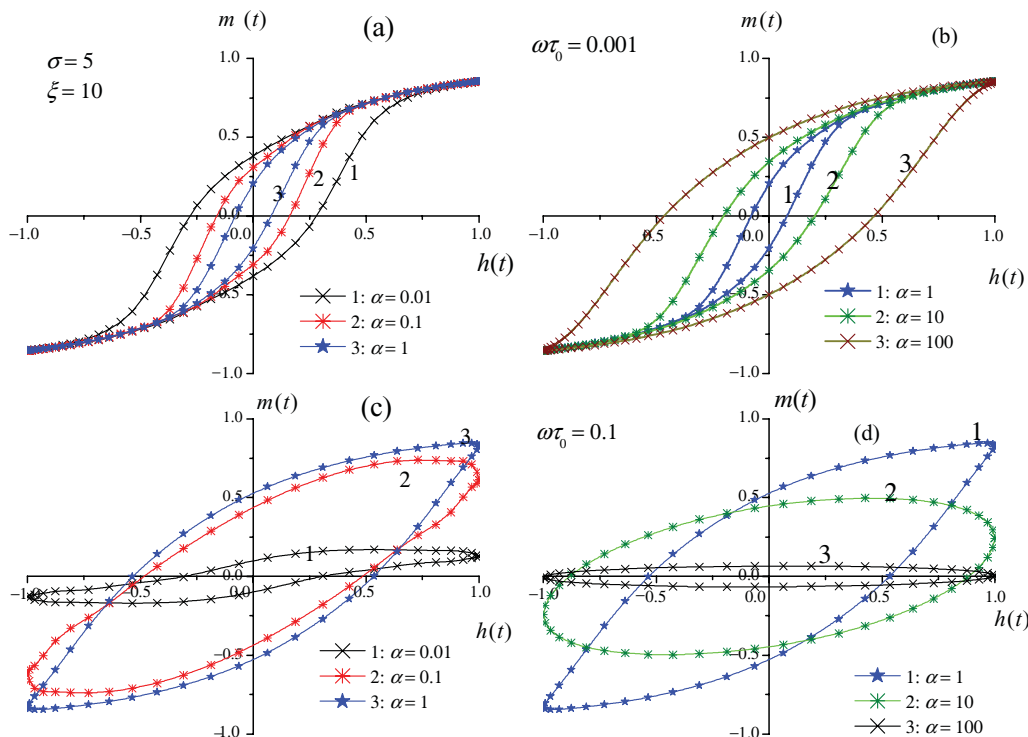


FIG. 1. (Color online) DMH loops [$m(t) = M_H(t)/M_S$ vs $h(t) = (\xi/2\sigma) \cos \omega t$] at quasistatic and intermediate frequencies for various values of the damping parameter α .

be understood via the plot of loop area vs α (Fig. 2), where a minimum is obtained for $\alpha \approx 1$ since under quasiadiabatic changes of the applied field (see curve 2 in Fig. 2), the coercivity may be within the Néel criterion $\omega\tau = 1$,^{9,18} where¹²

$$\tau \sim \tau_0 \frac{\sqrt{\pi}(1 + \alpha^2)}{\alpha\sigma^{1/2}(1 - h_{ef}^2)(1 - h_{ef})} e^{\sigma(1 - h_{ef})^2}, \quad (10)$$

and $h_{ef} = \xi/(2\sqrt{2}\sigma)$ is an ac field parameter, leading to a (transcendental) equation for the coercive force similar in form to that given by Sharrock.^{16,19} This procedure is, however, restricted to moderate to low temperatures¹⁶ because at higher temperatures, such an equation may not have a physically

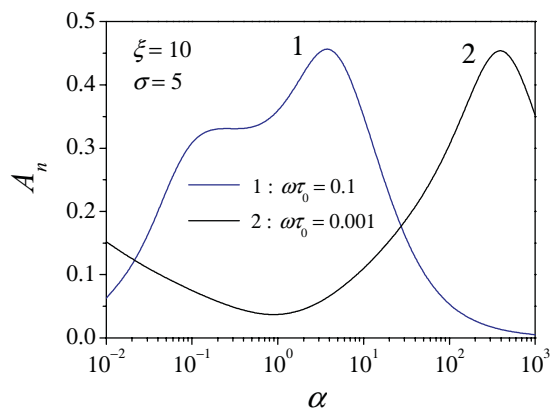


FIG. 2. (Color online) DMH loop area vs the damping parameter at quasistatic and intermediate frequencies.

meaningful solution. We may use these results for an assembly of randomly oriented particles to qualitatively estimate the coercive force because the relaxation time averaged over all easy-axis orientations is a minimum at $\alpha \approx 1$. However, on increasing the frequency by two orders of magnitude (see Figs. 1(c) and 1(d) and curve 1 in Fig. 2), we may perceive a different qualitative behavior of the DMH with damping because the coercivity now increases with increasing α . In effect, in this intermediate frequency range, the field variations compete with thermal agitation. Then, the effective reversal time is no longer given by Eq. (7), because the crossover between very low damping and intermediate to high damping is shifted to smaller α , meaning that gyroscopic effects can no longer be ignored in the DMH process. The remanent field and coercive force are, for low damping, much smaller than the Stoner-Wohlfarth values. However, they again grow as the damping increases until α reaches its maximum α_{cr} (Fig. 2), where the “kinetic freezing” regime is encountered. For $\alpha < \alpha_{cr}$, the DMH loops become quasi-elliptic.

Yet another new feature that has been ignored in previous studies^{4-7,10,16} is the damping dependence of the DMH at FMR frequencies. Here, DMH is encountered due to the *resonant* behavior of the nonlinear response (see Fig. 3). Therefore, such a regime may be termed the “resonant” regime, leading also to the concept of *resonant switching* of the magnetization. Here, the magnetization may be advantageously switched, because the field required to reverse the magnetization is much smaller than the quasistatic coercive force. Now for moderate ac fields, the DMH loops have an ellipsoidal shape (see Fig. 4), so that we may again infer that only a few harmonics actually contribute to the nonlinear response. In

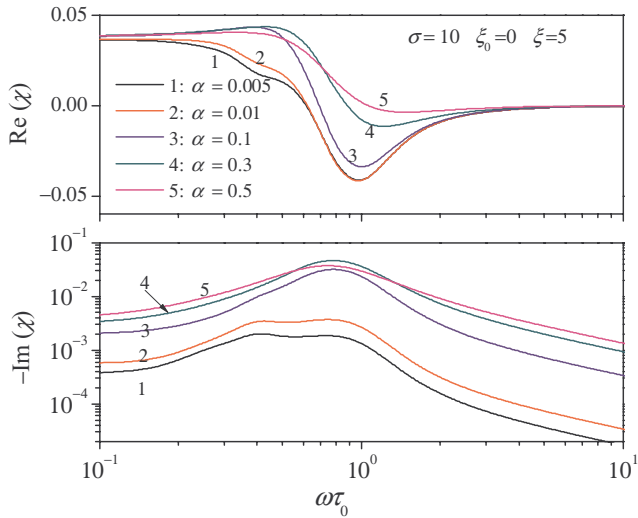


FIG. 3. (Color online) Real and imaginary parts of $\chi(\omega) = 2m_1/\xi$ vs $\omega\tau_0$ in the FMR region.

strong ac fields, the FMR peak and DMH loop area decrease substantially.¹⁵ In Fig. 5, the behavior of the resonant DMH loop vs damping is shown. For low damping, $\alpha \ll 1$, and high frequencies, $\omega \geq \omega_{\text{FMR}}$, the coercive force and remanence are small, and the system of single-domain ferromagnetic particles has *diamagnetic-like behavior*, in the sense that the largest *positive* value of the magnetization is attained at *negative* values of the field and vice versa, in contrast to the low-frequency behavior. Just as with linear response, in the vicinity of the FMR absorption peak, the orientation of the DMH loops depends on the phase lag $\Delta\phi$ between $M_H(t)$ and $H(t)$, which may exceed $\pi/2$ ($\Delta\phi$ being strongly damping dependent). Obviously, this effect does not exist at low and intermediate frequencies, where $\Delta\phi$ is always less than $\pi/2$. On increasing α from very low values, the loop area increases as the Q factor of the resonance decreases. This happens as the FMR peak merges with the broadband intermediate frequency “intrawell” peak.¹⁷ Here, the loop area passes through a maximum at some α_{cr} value. Then, as α is increased further,

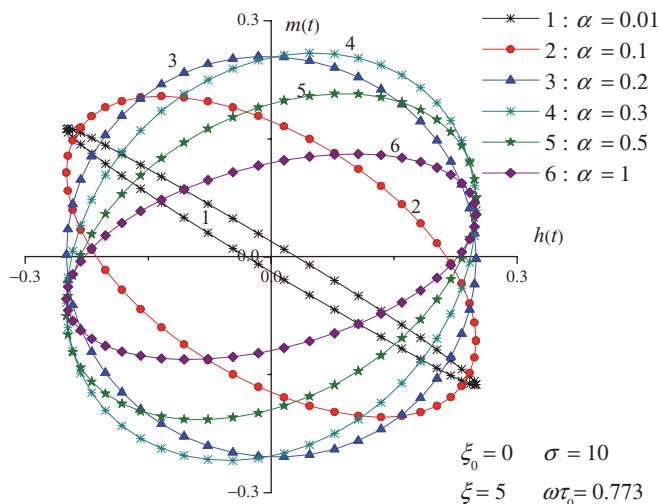


FIG. 4. (Color online) Resonant DMH loops for various values of the damping parameter α .

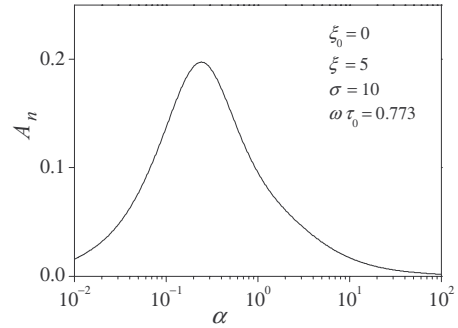


FIG. 5. Area of the resonant DMH loop vs the damping parameter α .

the kinetic freezing regime progressively appears. Indeed, that regime occurring in the FMR frequency region is analogous to that characteristic of a driven *overdamped* nonlinear oscillator. We note that, since, in practical applications, the resonant DMH loop area is smaller than the DMH in the quasistatic regime, the heat generated by the magnetic system is smaller in that regime. Resonant DMH occurs in a frequency band that is much narrower than that of the quasistatic regime because in that regime, the magnetization behaves like a nonlinear dash pot; in contrast, in the resonant regime (for given α), the magnetization behavior is analogous to that of a driven *underdamped* nonlinear oscillator. Since the resonant DMH occurs at very high (GHz) frequencies, the magnetization switching may be termed *ultrafast*, since the behavior of the reversal rate of the magnetization is mostly governed by the frequency of the external driving field, or equivalently, the rate of change of the applied field amplitude.

To conclude, we have shown that the DMH loops and absorption power of magnetic nanoparticle assemblies *strongly depend on damping* in all frequency ranges. In particular, we have shown that at low frequencies, the DMH loops exhibit a pronounced damping dependence due to *coupling of the thermally activated magnetization reversal mode with the precessional modes* of the magnetization via the driving ac field. Furthermore, the *damping dependence of the DMH that occurs in the FMR frequency range* may be used to model ultrafast switching of the magnetization in nanomagnets following an ultrafast change in the applied field. The predicted damping dependence of the DMH may be important in practical applications (magnetic information storage, hyperthermia) for which the parameters of the DMH loop are of utmost importance.¹⁶

ACKNOWLEDGMENTS

This work was supported by the Agence Nationale de la Recherche, France (Project DYSC No. ANR-08-P147-36) and by the European Community (Programme FP7, project DMH, No. 295196). We thank Yu. L. Raikher for useful discussions and comments.

APPENDIX: MATRIX CONTINUED FRACTION SOLUTION

As shown in Ref. 17a, the stationary ac nonlinear response can be calculated from the formally exact matrix continued

fraction solution

$$\begin{pmatrix} \vdots \\ \mathbf{c}_1^{-2} \\ \mathbf{c}_1^{-1} \\ \mathbf{c}_1^0 \\ \mathbf{c}_1^1 \\ \mathbf{c}_1^2 \\ \vdots \end{pmatrix} = \frac{-1}{\sqrt{4\pi}} \mathbf{S}_1 \cdot \begin{pmatrix} \vdots \\ \mathbf{0} \\ \mathbf{p}_1^- \\ \mathbf{q}_1^- \\ \mathbf{p}_1^- \\ \mathbf{0} \\ \vdots \end{pmatrix}, \quad (\text{A1})$$

where the infinite matrix continued fraction \mathbf{S}_1 is defined by the recurrence equation

$$\mathbf{S}_n = -[\mathbf{Q}_n + \mathbf{Q}_n^+ \mathbf{S}_{n+1} \mathbf{Q}_n^-]^{-1},$$

the three-diagonal supermatrixes \mathbf{Q}_n and \mathbf{Q}_n^\pm are given explicitly in Ref. 17a, and the column vectors \mathbf{c}_1^k , \mathbf{p}_1^- , and \mathbf{q}_1^- are defined as

$$\mathbf{c}_1^k = \begin{pmatrix} c_{2,-2}^k \\ c_{2,-1}^k \\ c_{2,0}^k \\ c_{2,1}^k \\ c_{2,2}^k \\ c_{1,-1}^k \\ c_{1,0}^k \\ c_{1,1}^k \end{pmatrix}, \quad \mathbf{q}_1^- = \begin{pmatrix} 0 \\ 0 \\ \frac{2\sigma}{\sqrt{5}} \\ 0 \\ 0 \\ \frac{\xi_0 \sin \psi}{\sqrt{6}} \\ \frac{\xi_0 \cos \psi}{\sqrt{3}} \\ -\frac{\xi_0 \sin \psi}{\sqrt{6}} \end{pmatrix}, \quad \mathbf{p}_1^- = \begin{pmatrix} 0 \\ 0 \\ 0 \\ 0 \\ 0 \\ \frac{\xi \sin \psi}{2\sqrt{6}} \\ \frac{\cos \psi \xi}{2\sqrt{3}} \\ -\frac{\xi \sin \psi}{2\sqrt{6}} \end{pmatrix}.$$

Here, $c_{l,m}^k$ are coefficients in the Fourier time series Eq. (4). Clearly, Eq. (A1) yields all the Fourier amplitudes required for the calculation of $M_H(t)$ in Eq. (3) and, hence, the DMH.

For an assembly of randomly oriented noninteracting uniaxial particles, in the calculation of the averages \overline{m}_1^k in Eq. (3) using Gaussian quadratures,²⁰ we only require (due to cylindrical symmetry about the Z axis)¹⁵

$$\overline{m}_1^k = \int_0^{\pi/2} m_1^k(\psi) \sin \psi d\psi = \frac{\pi}{4} \sum_{i=1}^n w_i m_1^k(\psi_i) \sin \psi_i,$$

where²⁰

$$w_i = \frac{2(1-x_i^2)}{[(n+1)P_{n+1}(x_i)]^2}, \quad \psi_i = \frac{\pi}{4}(x_i + 1),$$

and x_i is the i th root of the Legendre polynomial $P_n(x)$.¹⁹

For very low damping, $\alpha < 0.005$, the method is difficult to apply because the matrixes involved become ill conditioned, so that numerical inversions are no longer possible. The problem of convergence of matrix continued fractions is discussed in detail by Risken.²¹

*kalmykov@univ-perp.fr

¹R. Hergt, R. Hiergeist, M. Zeisberger, G. Glockl, W. Weitschies, L. P. Ramirez, I. Hilger, and W. A. Kaiser, *J. Magn. Magn. Mater.* **280**, 358 (2004); S. Dutz, R. Hergt, J. Mürbe, R. Müller, M. Zeisberger, W. Andrä, J. Töpfer, and M. E. Bellemann, *ibid.* **308**, 305 (2007); Y. Xu, M. Mahmood, Z. Li, E. Dervishi, S. Trigwell, V. P. Zharov, N. Ali, V. Saini, A. R. Biris, D. Lupu, D. Boldor, and A. S. Biris, *Nanotechnology* **19**, 435 (2008); B. E. Kashevsky, V. E. Agabekov, S. B. Kashevsky, K. A. Kekalo, E. Yu. Manina, I. V. Prokhorov, and V. S. Ulashchik, *Particuology* **6**, 322 (2008).

²J. P. Fortin, C. Wilhelm, J. Servais, C. Ménager, J. C. Bacri, and F. Gazeau, *JACS* **129**, 2628 (2007); J. P. Fortin, F. Gazeau, and

C. Wilhelm, *Eur. Biophys. J.* **37**, 223 (2008); L. M. Lacroix, R. Bel Malaki, J. Carrey, S. Lachaize, M. Respaud, G. F. Goya, and B. Chaudret, *J. Appl. Phys.* **105**, 023911 (2009).

³Q. A. Pankhurst, N. K. T. Thanh, S. K. Jones, and J. Dobson, *J. Phys. D: Appl. Phys.* **42**, 224001 (2009).

⁴V. A. Ignatchenko and R. S. Gekht, *Sov. Phys. JETP* **40**, 750 (1975).

⁵J. J. Lu, J. H. Huang, and I. Klik, *J. Appl. Phys.* **76**, 1726 (1994); V. Franco and A. Conde, *J. Magn. Magn. Mater.* **278**, 28 (2004); C. Tannous and J. Gieraltowski, *Physica B* **403**, 3578 (2008).

⁶Yu. L. Raikher, V. I. Stepanov, and R. Perzynski, *Physica B* **343**, 262 (2004); Yu. L. Raikher and V. I. Stepanov, *J. Magn. Magn. Mater.* **300**, e311 (2006).

- ⁷N. A. Usov and Yu. B. Grebenshchikov, *J. Appl. Phys.* **105**, 043904 (2009); J. Carrey, B. Mehdaoui, and M. Respaud, *ibid.* **109**, 083921 (2011); B. Mehdaoui, J. Carrey, M. Stadler, A. Cornejo, C. Nayral, F. Delpeche, B. Chaudret, and M. Respaud, *Appl. Phys. Lett.* **100**, 052403 (2012).
- ⁸W. F. Brown Jr., *Phys. Rev.* **130**, 1677 (1963); *IEEE Trans. Mag. Magn.* **15**, 1196 (1979).
- ⁹L. Néel, *Ann. Géophys.* **5**, 99 (1949).
- ¹⁰I. Klik and L. Gunther, *J. Stat. Phys.* **60**, 473 (1990).
- ¹¹Yu. L. Raikher and V. I. Stepanov, *Adv. Chem. Phys.* **129**, 419 (2004).
- ¹²P. M. Déjardin and Yu. P. Kalmykov, *J. Appl. Phys.* **106**, 123908 (2009); *J. Magn. Magn. Mater.* **322**, 3112 (2010); P. M. Déjardin, Yu. P. Kalmykov, B. E. Kashevsky, H. El Mrabti, I. S. Poperechny, Yu. L. Raikher, and S. V. Titov, *J. Appl. Phys.* **107**, 073914 (2010).
- ¹³J. L. Garcia-Palacios and P. Svedlindh, *Phys. Rev. Lett.* **85**, 3724 (2000).
- ¹⁴W. T. Coffey, D. S. F. Crothers, J. L. Dormann, L. J. Geoghegan, Yu. P. Kalmykov, J. T. Waldron, and A. W. Wickstead, *Phys. Rev. B* **52**, 15951 (1995); W. T. Coffey, D. S. F. Crothers, J. L. Dormann, L. J. Geoghegan, and E. C. Kennedy, *ibid.* **58**, 3249 (1998); Yu. P. Kalmykov and S. V. Titov, *Fiz. Tverd. Tela (St. Petersburg)* **40**, 1642 (1998); Yu. P. Kalmykov and S. V. Titov, *Phys. Solid State* **40**, 1492 (1998); W. T. Coffey, D. S. F. Crothers, Yu. P. Kalmykov, and S. V. Titov, *Phys. Rev. B* **64**, 012411 (2001).
- ¹⁵S. H. Thompson, G. Brown, A. D. Kuhnle, P. A. Rikvold, and M. A. Novotny, *Phys. Rev. B* **79**, 024429 (2009); S. H. Thompson, G. Brown, P. A. Rikvold, and M. A. Novotny, *J. Phys. Condens. Matter* **22**, 236001 (2010).
- ¹⁶I. S. Poperechny, Yu. L. Raikher, and V. I. Stepanov, *Phys. Rev. B* **82**, 174423 (2010).
- ¹⁷S. V. Titov, P. M. Déjardin, H. El Mrabti, and Yu. P. Kalmykov, *Phys. Rev. B* **82**, 100413(R) (2010); H. El Mrabti, S. V. Titov, P. M. Déjardin, and Yu. P. Kalmykov, *J. Appl. Phys.* **110**, 023901 (2011).
- ¹⁸A. Aharoni, *Phys. Rev.* **177**, 793 (1969).
- ¹⁹M. P. Sharrock, *J. Appl. Phys.* **76**, 6413 (1994).
- ²⁰M. Abramowitz and I. Stegun (eds.), *Handbook of Mathematical Functions* (Dover, New York, 1972).
- ²¹H. Risken, *The Fokker-Planck Equation*, 2nd ed. (Springer, Berlin, 1989).